s = factor defined as in Eq. 10 $[=\sigma/\rho_l g d_o^2]$
S = $(\pi/4)D^2\epsilon$, free cross-sectional area
V = superficial velocity, $m \cdot s^{-1}$
V' = absolute velocity, $m \cdot s^{-1}$
Y,Z = factors defined in Eq. 8

Greek Letters

α = empirical constant introduced in Eqs. 7 and 7a
α', α'' = empirical constants
α_b = nonideality factor, $0 \leq \alpha_b \leq 1$
β = total liquid saturation based on void volume
δ = dimensionless pressure drop $[=\Delta P/\rho g h]$
ϵ = porosity
γ_l = $[L/\rho_l)/(L/\rho_l) + (G/\rho_g)]$
μ = viscosity, $kg \cdot m^{-1} \cdot s^{-1}$
ρ = density, $kg \cdot m^{-3}$
σ = surface tension, $N \cdot m^{-1}$; standard deviation
τ = shear stress, $N \cdot m^{-2}$
ϕ = Energy dissipation, $N \cdot m \cdot s^{-1}$
ψ' = friction factor $[\Delta P/(\rho V^2/2)](d_p/h)$

Subscripts

f = frictional
g = gas
i = interface
l = liquid
lg = two-phase
s_p = single phase
w = water

Superscripts

o = single phase

LITERATURE CITED

Charpentier, J. C., C. Prost, and P. Le Goff, "Chute de pression pour des ecoulements a co-current et a contrecourant dans les colones a garnissage arrose: comparison avee le garnissage noye," *Chem. Eng. Sci.*, **24**, 1777 (1969).

Ergun, S., "Fluid flow through packed columns," *Chem. Eng. Prog.*, **2**, 89 (1952).

Rao, V. G., "Study of the pressure drop and liquid holdup in gas-liquid concurrent downflow through packed beds," Ph.D. Thesis, IIT Madras (1979).

Sato, Y., T. Hirose, F. Takahashi, and M. Toda, "Pressure loss and liquid holdup in packed bed reactor with cocurrent gas-liquid downflow," *J. Chem. Eng. Japan*, **6**, 147 (1973).

Specchia, V., and G. Baldi, "Pressure drop and liquid holdup for two-phase concurrent flow in packed beds," *Chem. Eng. Sci.*, **32**, 515 (1977).

Sweeney, D. E., "A correlation for pressure drop in two-phase cocurrent flow in packed beds," *AIChE J.*, **13**, 663 (1967).

Manuscript received October 31, 1981; revision received May 3, and accepted May 28, 1982.

Part II: Experiment and Correlations

Two-phase pressure drop and dynamic and total liquid saturation are experimentally determined for air-water system under cocurrent downflow through packed beds using packings differing widely in geometry. The experimental data of the present study as well as that available in literature is satisfactorily correlated in terms of: (a) Lockhart-Martinelli parameters; and (b) the Reynolds numbers defined for the respective phases and the bed porosity, taking into account the flow behavior of the phases through the packed bed.

V. G. RAO, M. S. ANANTH and Y. B. G. VARMA

Department of Chemical Engineering
Indian Institute of Technology
Madras-600 036, India

SCOPE

Gas-liquid cocurrent downflow is commonly encountered in chemical engineering practice as, for example, in synthesis of chemicals, hydrogenation and hydrodesulpurization of petroleum products, waste water treatment etc. Several studies have been reported in literature for foaming and nonfoaming systems in respect to the flow pattern delineation, the two-phase pressure drop, and the total and dynamic liquid saturation. The correlations in respect to pressure drop and liquid saturation are either based on Lockhart-Martinelli concept or in terms of directly measurable variables or the corresponding dimensionless groups and cover the entire region of operation.

Although distinct flow regions have been identified and the flow interaction mechanism is different in each identified region, the fact has not been considered in detail in the earlier investigations in developing the correlations except for delineation of the flow into poor and high interaction regimes (Midoux et al., 1976; Specchia and Baldi, 1977). This aspect, which is found to be of importance from the theoretical study, is included in the present investigation to correlate the experimental data more satisfactorily.

CONCLUSIONS AND SIGNIFICANCE

The pressure drop and dynamic and total liquid saturation are the important parameters in the design of equipment for gas-liquid cocurrent downflow through packed beds which is of common use in chemical engineering practice. The system presents different flow pattern depending on the flow rates of the phases and the packing characteristics and thus gives rise to different contacting mechanism between the phases in the different regions of flow.

This aspect has been considered in the present study, while formulating the correlations for the two-phase pressure drop and liquid saturation separately for each identified flow region, viz., the gas-continuous flow, the pulse flow, and the dispersed bubble flow. The correlations are presented in terms of: (i)

TABLE 1. EXPERIMENTAL CORRELATIONS ON TWO-PHASE PRESSURE DROP BY EARLIER INVESTIGATION

Experiment	Correlation and Range of Validity
Air-Water Raschig Rings: 9 mm Spheres: 3,9 mm (Larkins et al., 1961)	$\log\left(\frac{\delta_{lg}}{\delta_l + \delta_g}\right) = \frac{0.416}{(\log \chi)^2 + 0.666}$; $0.05 < \chi < 30$
Air-Water Raschig Rings: 6,12,25 mm Intalox Saddles: 12,25 mm Berl Saddles: 12 mm (Wen et al., 1963)	$\left(\frac{\Delta P}{h}\right) flg = a(L-b)^c + d\ 10^{eL}\ G$
Air-Water Alumina: 7.5 to 8.1 mm (Turpin and Huntington, 1967)	$ln\ \psi_{lg} = 7.96 - 1.34\ ln\ Z + 0.0021\ (lnZ)^2 + 0.0078\ (lnZ)^3$ $\psi_{lg} \equiv \delta_{lg} d_e / 2V_g^2 \rho_g$; $0.2 < Z < 500$
Air-Water Spheres: 2.6 to 24.3 mm (Sato et al., 1973)	$\log\left(\frac{\delta_{lg}}{\delta_l + \delta_g}\right) = \frac{0.70}{[ln\ (\chi/1.2)]^2 + 1}$; $0.1 < \chi < 20$ $\varphi_l = 1.30 + 1.85\chi^{-0.85}$
Air-Hydrocarbons Spheres: 3 mm Cylinders: 1.8 × 6 mm 1.4 × 5 mm (Midoux et al., 1976)	a) Poor gas-liquid interaction: foaming and nonfoaming $\varphi_l = +\chi^{-1} + 1.14\ \chi^{-0.54}$; $0.1 < \chi < 80$ b) High gas-liquid interaction foaming $(\xi_{lg}/\xi_l)^{0.5} = 1 + (\chi')^{-1} + 6.55(\chi')^{-0.43}$; $0.05 < \chi' < 100$
Air-Water; Air-Glycerol Spheres: 6 mm Cylinders: 2.7 × 2.7 mm 5.4 × 5.4 mm (Specchia and Baldi, 1977)	a) Low interaction regime: $\delta_{lg} = K_l \frac{[1-\epsilon(1-\beta_s-\beta_d)]^2}{\epsilon^3(1-\beta_s-\beta_d)^3} \mu_g V_g + K_2 \frac{[1-\epsilon(1-\beta_s-\beta_d)]}{\epsilon^3(1-\beta_s-\beta_d)^3} \rho_g V_g^2$ b) High interaction regime: $ln\ \psi_{lg} = 7.82 - 1.30\ ln(Z/\Delta^{1.1}) - 0.0573\ [ln(Z/\Delta^{1.1})]^2$ $0.0016 < V_l < 0.025$; $0.011 < V_g < 2.46$ $0.001 < \mu_l < 0.005$; $810 < \rho_l < 1070$ $0.027 < \sigma_l < 0.072$; $0.7 < \rho_g < 1.2$
Air-Water Glass Spheres: 1.2, 2.6, 4.3 mm (Matsuura et al., 1977)	$\left(\frac{\Delta P}{h}\right) = 4 f_t \frac{\rho_l V^2}{2g_c d_p} \frac{1-\epsilon}{\epsilon^3 \beta_d^2/\beta_t}$; $4 < Re_t < 10^3$ $f_t = 1.2 \times 10^3\ Re_t^{-1.1}$
Air-Silicone oil Spheres: 1.6, 2.9 mm Extrudate: 0.8 mm (Clements and Schmidt, 1980)	$\frac{\left(\frac{\Delta P}{h}\right)_{lg}}{\left(\frac{\Delta p}{h}\right)_g} = 190\ \mu_l d_e \left(\frac{\epsilon}{1-\epsilon}\right)^3 \left(\frac{Re_g We}{Re_l}\right)^{-1/3}$ (The constant, 190, is for d_e (ft) and μ_l (lb_m·ft·h)

Lockhart-Martinelli parameters; and (ii) Reynolds numbers defined for the respective phases and the bed porosity.

The present correlations cover a wide range in experimental conditions of the present study as well as that reported by the earlier investigators and are found to match the experimental data with improved confidence limits.

Experimental data relating to cocurrent gas-liquid downflow in packed beds for foaming and nonfoaming systems have been reported in literature, though the air-water system was extensively studied in particular for the pressure drop, liquid saturation, and flow pattern of the phases. Related mass transfer and chemical reaction aspects have also been covered to a lesser detail. Excellent reviews pertaining to the topic in recent times are due to Satterfield (1975), Charpentier (1976), Hofmann (1978), Hirose (1978), Gianetto et al. (1978), Shah et al. (1978), and Van Landeghem (1980).

The significant contribution in respect to the delineation of the flow regions and their analysis was due to Sato et al. (1973), Charpentier and Favier (1975), Talmor (1977), and Gianetto et al. (1978). Gas-continuous (trickle flow and spray flow), pulse flow, pulsing/bubbling, and dispersed bubble flow are the identified flow regions for nonfoaming systems, whereas gas-continuous (trickle flow and spray flow), foaming flow, foaming pulse flow, and pulse flow are identified for foaming systems. The flow maps were presented in terms of superficial mass flow rates of the phases, either G vs. L (Weekman and Myers, 1964; Sato et al., 1973; Charpentier et al., 1969; Beimesch and Kessler, 1971; Satterfield, 1975; Hofmann, 1978) or L/G vs. G (Turpin and Huntington, 1967; Charpentier and Favier, 1975; Midoux et al., 1976; Charpentier, 1976; Morsi et al., 1978) or $(L/G)\lambda\psi$ vs. $G/\lambda\epsilon$ (Gianetto et al., 1978) or $v_g/(v_l + v_g)$ vs. $(v_l + v_g)^2/d_p g$ (Matsuura, 1979) or in terms of force ratio (Talmor, 1977). However, no predictive correlations for transition from one flow region to another have been reported in literature.

The correlations presented by the earlier investigators for the pressure drop, Table 1, can be classified into two groups. (i) Correlations based on Lockhart-Martinelli concept, originally proposed for two-phase flow in horizontal pipes, relating the dimensionless parameters (Lockhart and Martinelli, 1949)

$$\varphi_1 = (\delta_{1g}/\delta_1^0)^{1/2} \text{ and } \chi = (\delta_l^0/\delta_1^0)^{1/2}$$

TABLE 2. EXPERIMENTAL CORRELATIONS ON TOTAL AND DYNAMIC LIQUID HOLDUP BY EARLIER INVESTIGATION

Experiment	Correlation and Range of Validity
Air-Water Spheres: 6.4 to 22 mm Raschig Rings: 12.7 mm Broken Solids: 25.4 mm (Otake and Okada, 1953)	$\beta_d = 15.1\, Re^{0.676}\, Ga^{-0.44}\, (a_s d_p)^{-0.6};\ 10 < Re < 2{,}000$ $= 21.1\, Re^{0.51}\, Ga^{-0.44}\, (a_s d_p)^{-0.6};\ 0.01 < Re < 10$
Air-Water Raschig Rings: 9 mm Spheres: 3, 9 mm (Larkins et al., 1961)	$\log \beta_d = -0.774 + 0.525 \log\chi - 0.109\, (\log\chi)^2;\ 0.05 < \chi < 30$
Air-Water Alumina: 7.5 to 8.1 mm (Turpin and Huntington, 1967)	$\beta_d = 0.132\, (L/G)^{0.24} - 0.017;\ 1 < (L/G)^{0.24} < 6$
Air-Water Spheres: 4.8 mm (Hochman and Effron, 1969)	$\epsilon\beta_d = 0.00445\, Re_l^{0.76}$
Air-Hydrocarbon Spheres: 3 mm Cylinders: 1.6 × 1.6 mm 3.2 × 3.2 mm (Satterfield and Way, 1972)	$\beta_t = AV_l^{1/3}\mu_{\mu l}^{1/4} + B$
Air-Water Spheres: 2.6 to 24.3 mm (Sato et al., 1973)	$\epsilon\beta_t = 0.4\, \chi^{0.22}\, a_s^{1/3};\ 1 < \chi < 20$
Air-Water Cylinders: 1.8 × 6 mm 1.4 × 5 mm Spheres: 3 mm (Charpentier and Favier, 1975)	a) Spherical packing: $\log \beta_t = -0.28 + 0.175 \log \chi' - 0.047\, (\log \chi')^2;\ 0.05 < \chi' < 100$ b) Cylindrical packing: $\log \beta_t = -0.363 + 0.168 \log \chi' - 0.043 (\log \chi')^2;\ 0.05 < \chi' < 100$
Air-Water Spheres: 4.13 mm Catalyst: 2.91 mm β-Naphthol: 0.5 to 2.4 mm (Goto and Smith, 1975)	$\beta_d = 1.25\, Re_l^{0.676}\, Ga^{-0.44}\, a_s d_p;\ 10 < Re_1 < 200$
Air-Hydrocarbon Spheres: 3 mm Cylinders: 1.8 × 6 mm 1.4 × 5 mm (Midoux et al., 1976)	a) Poor gas-liquid interaction: foaming and non-foaming $\beta_t = 0.66\, \chi^{0.81}/(1 + 0.66\, \chi^{0.81});\ 0.1 < \chi < 80$ b) High gas-liquid interaction: foaming $\beta_t = 0.92\, (\chi')^{0.3}/[1 + 0.92 (\chi')^{0.3}];\ 0.05 < \chi' < 100$
Air-Silicone Oil Extrudate: 1.0, 1.9, 3.4 mm Cylinders: 1.37, 1.92, 2.13, 3.50 mm (Clements, 1976)	a) Nonfoaming systems: $\epsilon\beta_d = 0.111\, (We\, Re_g/Re_l)^{-0.034}$ b) Foaming systems: $\beta_d = 0.245\, (We\, Re_g/Re_l)^{-0.034}$
Air-Water; Air-Glycerol Spheres: 6 mm Cylinders: 2.7 × 2.7 mm 5.4 × 5.4 mm Raschig Rings: 6.4, 10.3, 22 mm (Specchia and Baldi, 1977)	a) Low interaction regime: foaming and non-foaming $\beta_d = 3.86\, Re_l^{0.545}\, (Ga')^{-0.42} (a_s d_p/\epsilon)^{0.65};\ 3 < Re_l < 470$ b) High interaction regime: nonfoaming $\beta_d = 0.125 (Z/\Delta^{1.1})^{-0.312} (a_s d_p/\epsilon)^{0.65};\ 1 < (Z/\Delta^{1.1}) < 500$ c) High interaction regime: foaming $\beta_d = 0.0616 (Z/\Delta^{1.1})^{-0.172} (a_s d_p/\epsilon)^{0.65}$
Air-Hydrocarbon Spherical Catalyst: 2.4 mm (Morsi et al., 1978)	$\beta_d = 0.86\, (L/19.9)^{-0.198} \log (\mu_l/80.8)$ $G < 0.01;\ L < 19.9;\ \mu_l < 90.8$ cp
Air-Water Glass Spheres: 1.2 to 4.3 mm (Matsuura et al., 1979)	$\beta_d = 13.5\, Re_l^{1/3}\, Ga_l^{-1/3} + 1.2\, Re_l Ga_l^{-1/2}$

These correlations necessitate the actual measurement or prediction of single-phase pressure losses at the same mass flow rates of the phases as in two-phase flow through the packed bed. The concept was used by Larkins et al. (1961), Sato et al. (1973), Weekman and Myers (1964), and in the modified form by Charpentier and coworkers (1971). (ii) Correlations relating the two-phase pressure drop directly to the measurable flow variables or the corresponding dimensionless numbers, as was due to Turpin and Huntington (1967). Midoux et al. (1976) and Specchia and Baldi (1977) modified the approach introducing: (a) low-interaction regime comprising of trickle flow; and (b) high-interaction regime consisting of all other flow regions to correlate the pressure drop.

It may, however, be noted that neither of the approaches considers the flow pattern of the phases in conjunction with the pressure drop and liquid saturation. This becomes important when one considers that the contacting mechanism between the phases differs in different flow regions. The pressure drop correlations due to Sato et al. (1973) and Specchia and Baldi (1977) may be used to predict the experimental data within ±30% for nonfoaming systems, whereas the correlation due to Charpentier et al. (1971) predicts the experimental data with similar accuracy for foaming systems.

The liquid saturation in two-phase gas-liquid downflow in packed beds was differently reported by the earlier investigators as total liquid saturation and dynamic liquid saturation, the latter depending on the method and duration of the collection of the liquid from the packed bed.

The total liquid saturation was satisfactorily related to the dimensionless parameter, χ, as with two-phase pressure drop, by Sato et al. (1973) incorporating an additional term to represent the specific surface area of the packing.

The dynamic liquid saturation was related by Turpin and Huntington (1967) to the mass flow rates of the phases, whereas Specchia and Baldi (1977) correlated the same to the two-phase pressure drop using a modified Gallileo number in the low in-

teraction regime. Specchia and Baldi (1977), however, related the dynamic liquid saturation for high interaction regime to $Z = Re_l^{1.167}/Re_g^{0.767}$, originally used by Turpin and Huntington (1967) to relate the two-phase pressure loss. The correlations relating the liquid saturation are presented in Table 2.

The fraction of the dynamic liquid saturation in the total liquid saturation was differently reported as ranging from 0.90 to 0.60 by different investigators, suggesting the need for separate correlations for the total and dynamic liquid saturation.

THE EXPERIMENT

The experimental setup, Figure 1, consisted of a perspex column of 92.4 mm i.d. with a packing height of 1,835 mm, with provision to feed air and water through a distributor at the top of the column; the movement of the phases being cocurrent downflow over the stationary packing. Water was pumped from a 200-L tank through low and high range flowmeters to feed into the distributor consisting of 32 copper tubes of 180 mm long, 4 mm i.d. spread over the column cross-section on a square pitch to ensure equal distribution of water. Air was drawn from a compressor through an air filter, a pressure regulator, control valves, and low/high flowmeters to feed into the distributor consisting of 37 copper tubes of 120 mm long, 4 mm i.d. placed alternately to the water-carrying tubes over the entire cross-section. The packing was supported on a 5-mm thick perforated brass sheet with 50% free area. The discharger at the bottom of the column consisted of two concentric perspex tubes with a brass conical bottom to facilitate the separation and discharge of the phases.

The quick-closing cock valves provided at the top and bottom of the column facilitated the simultaneous cutoff of the phases when desired. A beam balance was provided at the top to weigh the entire column with an accuracy of ±3 g for the measurement of the liquid saturation.

The total liquid Saturation, β_t, was obtained by weighing the entire column when under steady operation for known flow rates of the phases and subtracting from the same the dry weight of the column including the packings. The dynamic liquid saturation, β_d, was measured for different flow rates of the phases by measuring the volume of the liquid drained for 15 minutes after the inflow was stopped. The dynamic liquid saturation is defined as

$$\beta_d = \frac{\text{Volume of the Liquid Drained}}{\text{Total Void Volume of the Bed}}$$

The void volume of the bed was obtained by weighing the column with the dry packing and again weighing the column with packing filled with water to the level of the packing. The porosity, ϵ, is calculated from the total void volume and the volume of the packed column.

The static liquid saturation, β_s, was determined by subtracting the dynamic liquid saturation from the total liquid saturation.

For the measurement of the pressure drop, five measuring points were provided with longitudinal intervals of 150, 400, 500, 600, and 100 mm beginning from the top of the packing. For the use in correlations, however, the pressure drop per unit length of the packing in the middle section corresponding to 550 to 1,050 mm from the top of the packing was used. The flow pattern of the phases was visually observed. The following range of variables were covered in the present study.

Mass Liquid Flow Rate, L, $kg \cdot m^{-2} \cdot s^{-1}$: 4.13–99.1
Mass Gas Flow Rate, G, $kg \cdot m^{-2} \cdot s^{-1}$: 0.16–3.2

Packing Characteristics	Size, mm	d_p, mm	ϵ
Ceramic Cylinders	13.07 × 13.87	13.33	0.381
	8.18 × 7.91	8.09	0.373
Ceramic Spheres	6.72	6.72	0.373
	4.00	4.00	0.365
Rasching Rings	9.54	3.14	0.701
Berl Saddles	11.00	4.08	0.632

The experimental procedure in the present investigation aimed at: (i) the identification of the flow regions and the transition from one flow region to another; (ii) the measurement of the pressure drop; and (iii) the measurement of total and dynamic liquid saturation in the column.

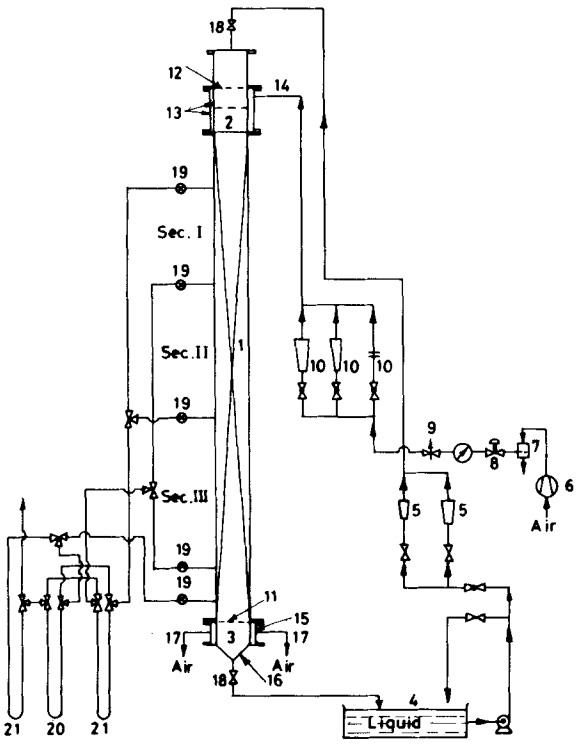

Figure 1. Schematic diagram of the experimental setup: 1. packed section; 2. distributor; 3. discharger; 4. 200-L tank; 5. low/high range flowmeters for water; 6. compressor; 7. air-filter; 8. pressure regulator; 9. control valve; 10. low/high range flowmeters for air; 11. grid plate; 12. brass plate; 13. concentric cylinders; 14. radial feed inlets for air; 15. concentric perspex tubes; 16. brass conical section; 17. outlet tubes for air; 18. quick-closing valves; 19. gas-liquid separators; 20. mercury manometer; 21. carbon tetrachloride manometers.

FLOW PATTERN OF THE PHASES

The following observations are made from the experimental data. The flow pattern of the phases identified in the present investigation correspond to those reported in literature, viz., trickle flow, spray flow, pulse flow, and dispersed bubble flow. The flow pattern essentially depends on the relative mass flow rates of the phases, whereas the flow boundary for a chosen type of flow is strongly influenced by the porosity of the bed. The higher the porosity, the smaller is the pulse flow region and the larger is the required flow rates of the phases for the onset of pulse flow in the packed column.

The transition from gas-continuous to pulse flow is strongly dependent on the packing size and porosity, though the transition from pulse flow to dispersed bubble flow is relatively unaltered by these variables. The experimental data of the present study and that of Sato et al. (1973) indicate that the flow pattern changes from gas-continuous to pulse flow at minimum flow rate of the phases of spherical packings of 6–8 mm diameter.

The flow pattern observed in the present study exhibits the trend noted by Sato et al. (1973) and confirm to the flow boundary given by Talmor (1977) for pulse flow. The experimental data, however, agree well with the flow map suggested by Gianetto et al. (1978).

Two-Phase Pressure Drop

The two-phase pressure drop is an important design parameter, as the throughput and mass transfer depend on the energy dissi-

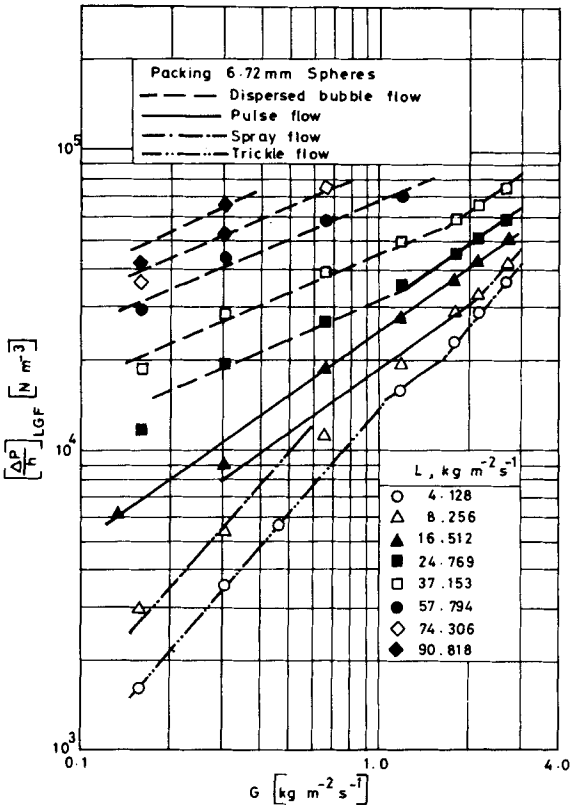

Figure 2. Typical variation in experimental two-phase pressure drop with mass flow rate of the phases for different flow regions.

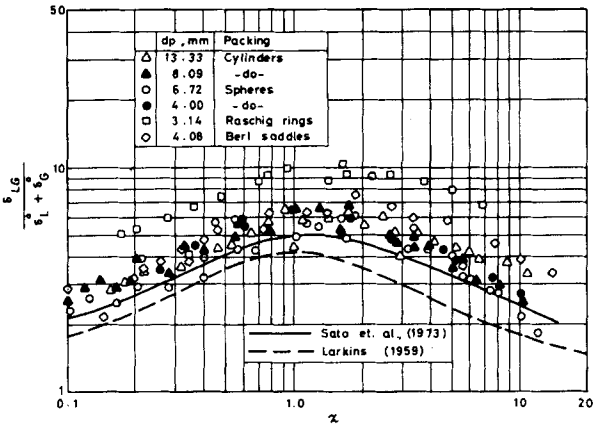

Figure 3. Comparison of the present experimental two-phase pressure drop data with correlation due to Larkins (1959) and Sato et al. (1973).

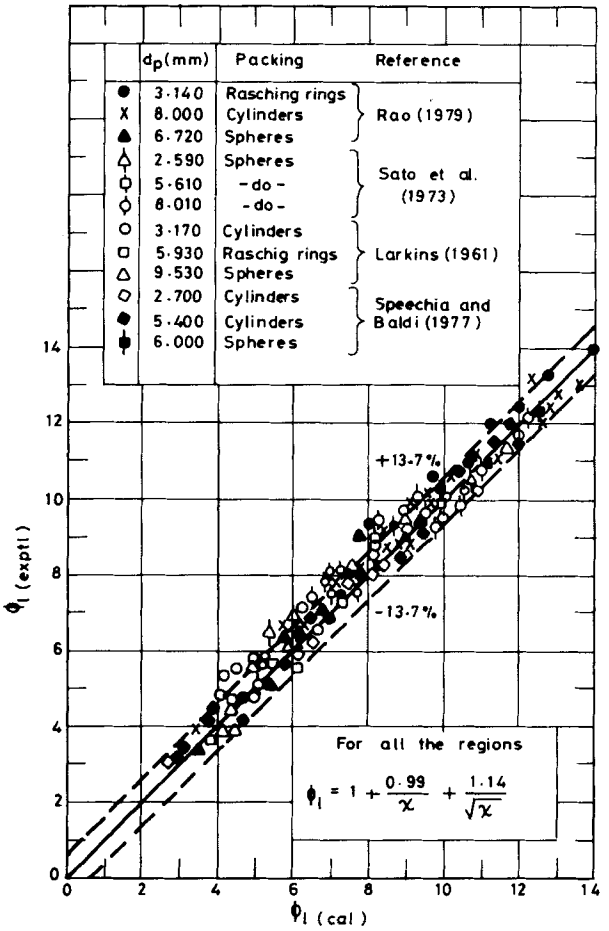

Figure 4. Comparison of experimental two-phase pressure drop data with the predicted values of pressure drop.

pation. Figure 2 shows typical variation of the two-phase pressure drop with a change in air and water flow rates. The following observations are made from the study.

The pressure drop per unit length varies along the length of the packing, decreasing from top to the bottom of the column. However, during the transitional flow pulse formation, ΔP_{lg} is found to be maximum at the bottom of the column, where the pulses begin to generate initially, and minimum near the top of the packing.

ΔP_{lg} is found to increase with increase in the mass flow rate of either of the phases, and decrease with increase in either effective particle diameter or porosity of the bed. The variation in the pressure drop with a variation in the gas rate, keeping the liquid rate constant, shows a maximum of three identified flow patterns, viz., gas-continuous, pulse, and dispersed bubble flow. Corresponding to each of the three flow patterns, lines of the three different slopes are obtained, indicating that a single equation relating the two-phase frictional pressure drop to the operating variables may be inadequate. (The lines representing trickle flow and spray flow have identical slopes in Figure 2.) An analysis of the experimental data of Larkins (1959) shows similar trend.

The transition from one flow pattern to another, for example, from dispersed bubble flow to pulse flow, occurs at high gas rate when the liquid rate is increased. However, at very high liquid rates, the transition from dispersed bubble flow to pulse flow is almost independent of the gas rate, which is also indicated in the flow maps.

EXPERIMENTAL DATA VS. CORRELATIONS OF EARLIER INVESTIGATIONS

The two-phase pressure drop was correlated by the earlier investigators in terms of: (i) the dimensionless parameter, χ or χ' or (ii) the flow rates of the phases or the corresponding dimensionless groups.

Sato et al. (1973) related the two-phase pressure drop to the Lockhart-Martinelli parameter, noting, however, that the curve is symmetrical at $\chi = 1.2$ instead of at $\chi = 1.0$ as was observed by Larkins (1959). Figure 3 compares the experimental data with the aforementioned correlations, showing that the predicted pressure loss is less compared to the experimental data.

Charpentier and coworkers (1968, 1969) obtained frictional pressure loss using both momentum and energy balances and observed that the modified Lockhart-Martinelli parameter, χ' defined as

$$\chi' = [(L/G)/(1/\rho_g g)(\Delta P/h)_g^o + 1]^{1/2} \qquad (1)$$

based on the energy balance, correlated the experimental data better than the parameter, χ. Subsequently, Midoux et al. (1976), studying foaming and nonfoaming hydrocarbon systems, suggested

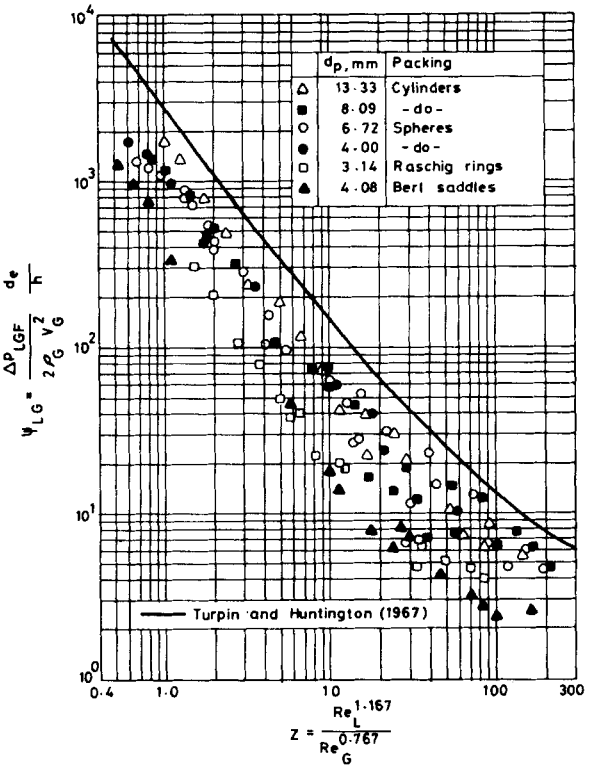

Figure 5. Comparison of the present experimental two-phase pressure drop data with the correlation due to Turpin and Huntington (1967).

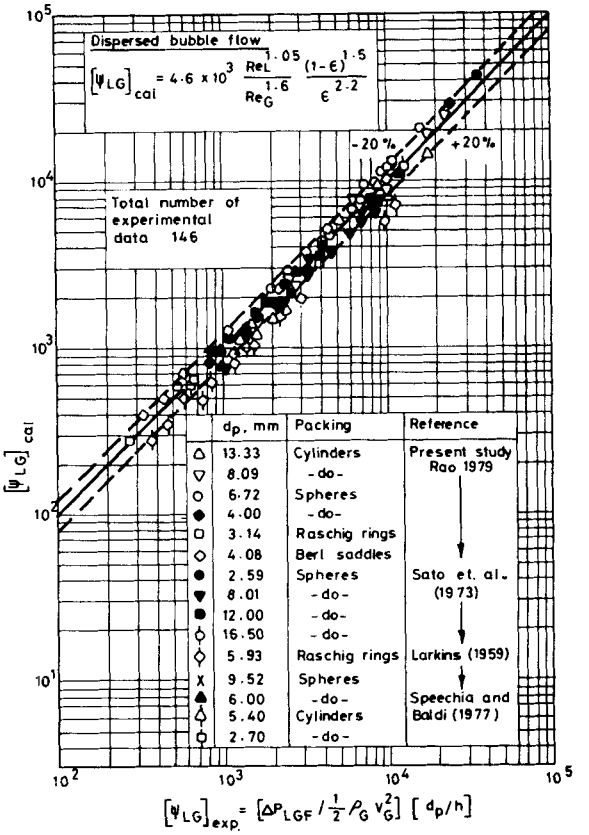

Figure 6. Comparison of the experimental two-phase pressure drop data with the present correlation for dispersed bubble flow.

two sets of correlations for poor and high gas-liquid interaction regimes, respectively. The experimental data of the present study and that of earlier investigators is, however, found to correlate satisfactorily, Figure 4, using the equation

$$\varphi_1 = 1 + \frac{0.99}{\chi} + \frac{1.14}{\sqrt{\chi}} \tag{2}$$

which is similar to that given by Midoux et al. (1976) for poor gas-liquid interaction regime.

Turpin and Huntington (1967) correlated the two-phase friction factor as a polynomial in *ln* Z. Figure 5 compares the experimental data with the correlation due to Turpin and Huntington (1967) showing that the correlation predicts higher pressure drop than the experiment, the deviation being significantly large for the data obtained using Raschig rings.

Specchia and Baldi (1977) calculated the free area available for gas flow, taking into account the dynamic and static liquid saturation, and related the two-phase pressure drop using Ergun-type equation in the poor interaction regime. The authors used a combination of the parameter Z defined by Turpin and Huntington (1967) and the parameter Δ introduced by Charpentier and Favier (1975) to relate the two-phase pressure loss for the high interaction regime. Clements and Schmidt (1980a) related the pressured drop to Weber and Reynolds numbers.

CORRELATION

The experimental data of the present study and that reported in literature (Larkins, 1959) indicate that the pressure drop is strongly influenced by the flow pattern of the phases. Since the controlling hydrodynamic mechanism is different for the different flow pattern, considering the flow pattern while correlating the data for the pressure loss seems to be appropriate. Though this was noted by Charpentier et al. (1969), Hofmann (1978) and Gianetto et al. (1978), no attempt was, however, made by the authors to relate the two-phase pressure loss separately for each identified flow region.

The experimental data of the present study as well as that reported by Larkins (1959), Sato et al. (1973), and Specchia and Baldi (1977) barring the data at the transition from one flow region to another are satisfactorily correlated, Figures 6 to 8, for each identified flow region, satisfying the following equations:

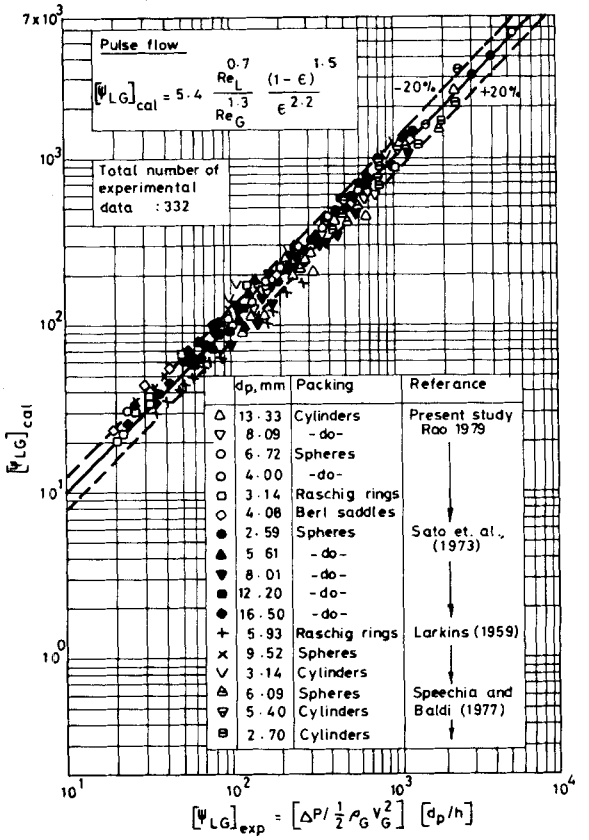

Figure 7. Comparison of the experimental two-phase pressure drop data with the present correlation for pulse flow.

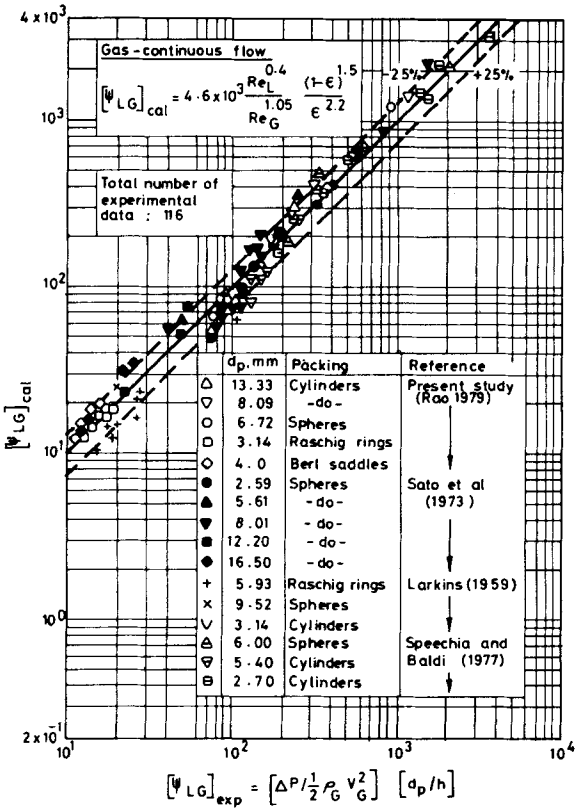

Figure 8. Comparison of the experimental two-phase pressure drop data with the present correlation for gas-continuous flow.

Gas-Continuous Flow (Trickle Flow and Spray Flow):

$$\psi_{1g} = 4.6 \times 10^3 \frac{Re_l^{0.4}}{Re_g^{1.05}} \eta^{0.75};\ \sigma = 0.15 \tag{3}$$

Pulse Flow:

$$\psi_{1g} = 5.4 \times 10^3 \frac{Re_l^{0.7}}{Re_g^{1.3}} \eta^{0.75};\ \sigma = 0.20 \tag{4}$$

Dispersed Bubble Flow:

$$\psi_{1g} = 4.6 \times 10^3 \frac{Re_l^{1.05}}{Re_g^{1.6}} \eta^{0.75};\ \sigma = 0.20 \tag{5}$$

where

$$\psi_{1g} \equiv \left[\frac{\Delta P_{flg}}{\frac{1}{2}\rho_g V_g^2}\right]\left[\frac{d_p}{h}\right];\ \eta = \frac{(1-\epsilon)^2}{\epsilon^3}$$

Equations 3 to 5 enable the prediction of ΔP_{flg}, once the flow region is identified, using the directly measurable values, rather than through the single-phase pressure losses, ΔP^o_{fl} and ΔP^o_{fg} whose measurement or estimation is relatively poor in its reproducibility.

LIQUID SATURATION

The liquid saturation in two-phase flow is one of the important measures of contacting effectiveness between the liquid and solid phases. The total liquid saturation, β_o, in a packed bed may be divided into: (i) that present within the pores of the particles, β_i; and (ii) that held in the interstices between the particles, β_t. The external liquid saturation β_t, is further subdivided into: (iii) the dynamic liquid saturation, β_d corresponding to the liquid drained in a specified time, say 15 min, from the packed bed after the inflow is stopped; and (iv) the static liquid saturation, β_s, corresponding to that remaining in the bed for a long time. The dynamic and static liquid saturation, β_d and β_s, do not necessarily correspond to: (v) the active liquid saturation, β_a; and (vi) the inactive liquid saturation, β_r, which are observed during the continuous operation of the column and can only be obtained through tracer technique. β_r is, however, always less than β_s and may be as low as $\frac{1}{4}$th of the static liquid saturation.

The external liquid saturation, β_t, in trickle flow consists of: (i) the thin liquid film flowing over the packing; (ii) the rivulet that does not spread into a film; (iii) the liquid drop suspended in the gas phase; and (iv) the stagnant liquid at the contact between particles. It is found from the experimental data that β_t increases with increase in the liquid flow rate, but decreases with increase in the air rate. The latter is attributed to the decrease in rivulets since the contribution of the suspended drops remains unchanged and that of the liquid film even increases slightly (Hofmann, 1978).

EXPERIMENTAL DATA VS. EARLIER CORRELATIONS

The total and dynamic liquid saturation in two-phase flow through packed beds was correlated by the earlier investigators in terms of either the dimensionless parameter χ or χ' or the flow rates of the phases or the corresponding dimensionless groups (Table 2).

Sato et al. (1973) noticed a significant dependence of β_t on specific surface area, which is in agreement with the observation of the present study, wherein β_t is found to increase with a decrease in the effective particle diameter of the packing. Charpentier et al. (1968, 1969) measured the total liquid saturation, analyzed the texture of the liquid film in terms of "films, rivulets and drops," and divided β_t into these component parts to present their results graphically.

Charpentier and Favier (1975) reported that the noncapillary liquid saturation (β_t in the present case) was better correlated by modified Lockhart-Martinelli parameter χ' rather than by χ. Subsequently, Midoux et al. (1976) suggested two sets of correlations for poor and high gas-liquid interaction regimes based on their data for foaming and nonfoaming systems.

A comparison of the experimental data of the present study with

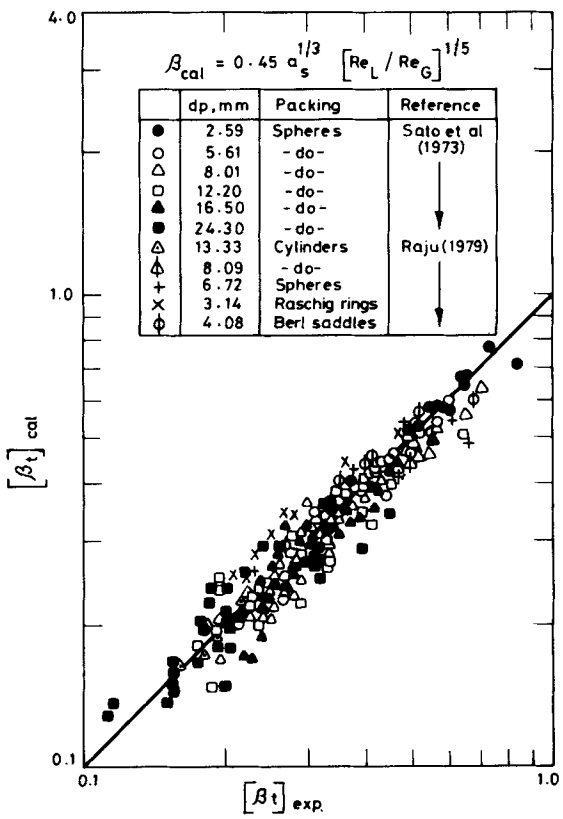

Figure 9. Comparison of the experimental and predicted total liquid saturation.

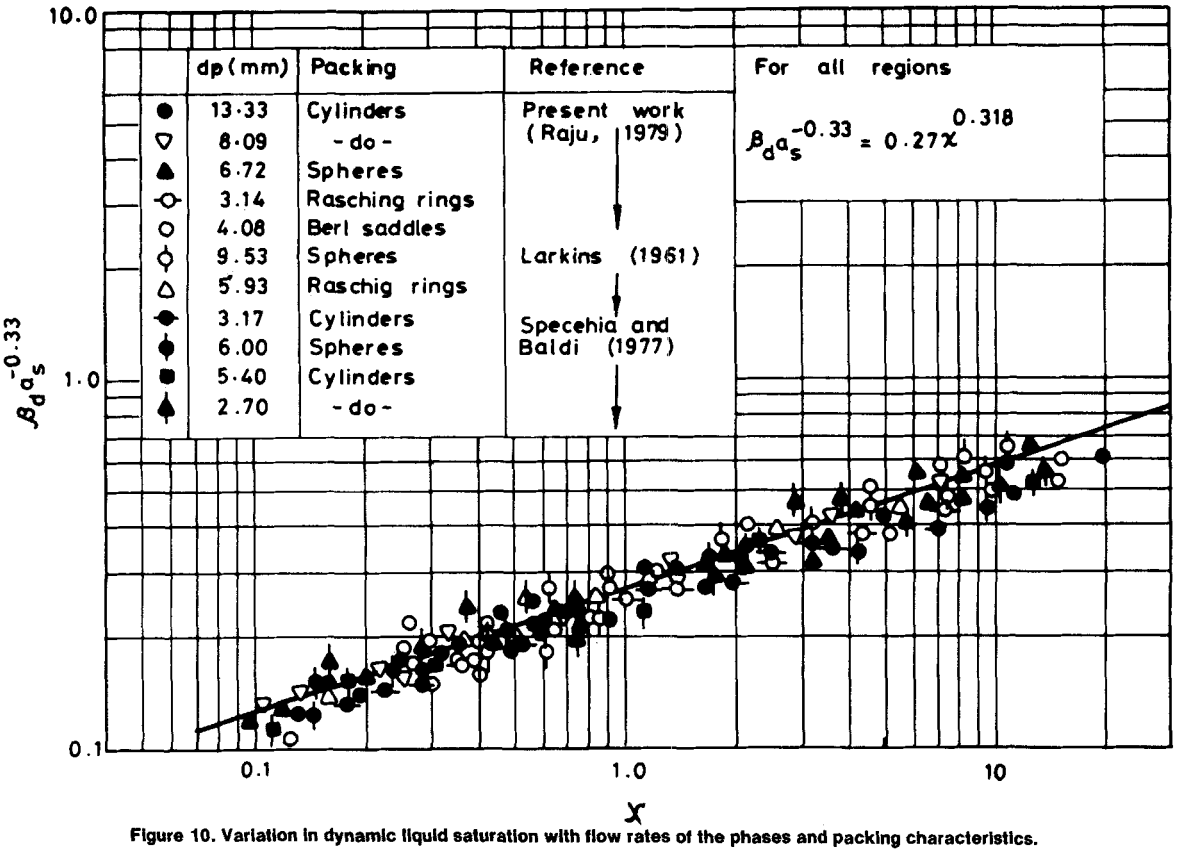

Figure 10. Variation in dynamic liquid saturation with flow rates of the phases and packing characteristics.

the correlations due to Sato et al. (1973) and Charpentier and Favier (1975) shows that the correspondence of the data with the latter correlation is relatively poor. Schwartz et al. (1976) compared their data obtained using 6-mm diameter porous and nonporous alumina packings with the aforementioned correlations and noted that the correlations underestimated the liquid saturation by 25 to 40%. This discrepancy is perhaps due to the fact that their data were primarily in the low interaction regime while the correlations emphasize the high interaction regime.

The experimental data of the present study and that due to Sato et al. (1973) is correlated in terms of χ and Reynolds numbers based on the flow rates of the phases as follows:

$$\beta_t a_s^{-1/3} = A\chi^B \tag{6}$$

$$\beta_t a_s^{-1/3} = c(Re_l/Re_g)^D \tag{7}$$

The correlating constants A to D along with the standard deviation, σ, are tabulated as below for the entire region of operation and for each flow region.

	A	B	σ	C	D	σ
Gas Continuous Flow	0.40	0.23	14.0	0.35	0.14	0.09
Pulse Flow	0.40	0.27	10.1	0.35	0.20	0.10
Dispersed Bubble Flow	0.38	0.28	11.9	0.35	0.26	0.09
Entire Region	0.40	0.22	17.6	0.45	0.20	0.14

Equation 7, resulting in satisfactory correlation of the data, Figure 9, is advantageous as it relates the total liquid saturation to the flow variables, instead to the liquid and gas pressure losses as in Eq. 6.

DYNAMIC LIQUID SATURATION

The dynamic liquid saturation, β_d, as with β_t, increases with increase in the liquid flow rate and a decrease in the gas rate. β_d is found to be less for packing such as Raschig rings and Berl saddles that result in greater porosity for the bed.

The experimental data of the present study and that due to

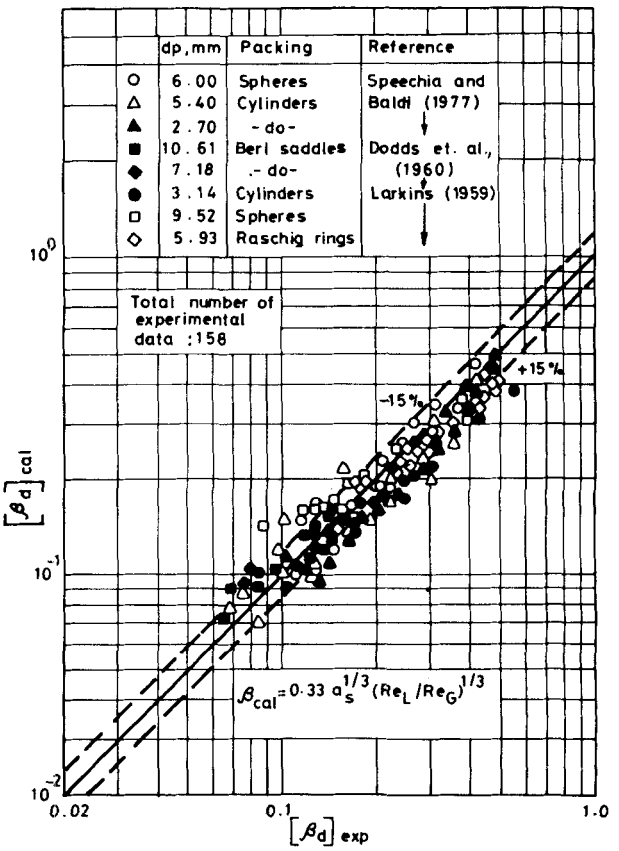

Figure 11. Comparison of the dynamic liquid saturation data of literature with the present correlation.

Larkins et al. (1961) and Specchia and Baldi (1977) is satisfactorily correlated as follows (Figure 10):

$$\beta_d a_s^{-1/3} = 0.27\,\chi^{0.318} \tag{8}$$

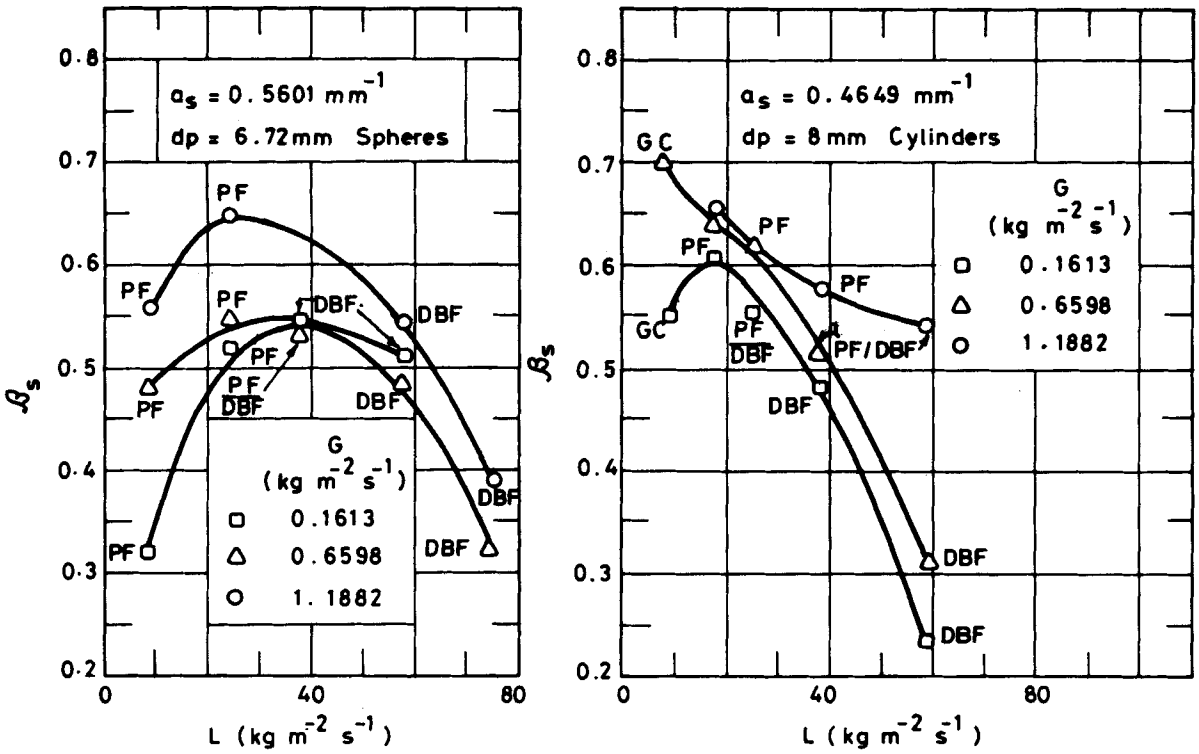

Figure 12. Typical variation of static liquid saturation with the mass flow rates of the phases.

The experimental data of the earlier investigators are also satisfactorily correlated for the entire range of operation in terms of Reynolds number based on the flow rates of the phases (Figure 11):

$$\beta_d a_s^{-1/3} = 0.33\,(Re_l/Re_g)^{1/3} \tag{9}$$

Turpin, and Huntington (1967) related β_d to the ratio of the flow rates of the phases, whereas Clements (1978, 1980b) correlated the dynamic liquid saturation in terms of Weber and Reynolds numbers separately for foaming and nonfoaming systems.

Specchia and Baldi (1977) divided the experimental data into two hydrodynamic regions, viz., poor and high interaction regimes, and related β_d separately for each of the regimes.

The equation for the poor interaction regime is of the type given by Otake and Okada (1953) for broken solids and Raschig rings. The correlation for high interaction regime, however, takes into account the two parameters Z and Δ, originally defined by Turpin and Huntington (1967) and Charpentier and Favier (1975), respectively. The data of the present study and those of Larkins et al. (1961) and Specchia and Baldi (1977) are satisfactorily correlated in terms of Z for the entire range of operation with a standard deviation of $\sigma = 0.13$:

$$\beta_d \left(\frac{1-\epsilon}{\epsilon}\right)^{-0.125} = 0.54\,Z^{-0.315} \tag{10}$$

Matsuura et al. (1979) considered the interactions among the liquid saturation, the pressure gradient, and the liquid flow rate for the gravity-viscosity and the gravity-inertia regions to relate the dynamic liquid saturation in terms of the static pressure gradient.

STATIC LIQUID SATURATION

The static liquid saturation, β_s, depends on the liquid physical properties and the particle size, shape and wettability. Mersmann (1965) correlated β_s for nonporous packing to Eötvos number, $E\ddot{o} \equiv \rho_l g d_p^2/\sigma$ which is the ratio of gravitational and surface tension forces. At $E\ddot{o} < 1$, β_s is independent of $E\ddot{o}$; at $5 < E\ddot{o} < 50$, β_s decreases with $\sqrt{E\ddot{o}}$; for $E\ddot{o} > 100$, β_s decreases with $E\ddot{o}^{-1}$. Charpentier et al. (1968) presented graphically β_s as function of $E\ddot{o}$.

Mersmann (1975) correlated the data for various systems in terms of Bond number as:

$$\beta_s = 3.7 \times 10^{-2}\,(\rho_l g/\sigma a_s^2)^n \tag{11}$$

where $n = -0.07$ for $Bn < 1$ and $n = -0.65$ for $Bn > 1$.

The experimental data of the present study show that β_s increases with increase in liquid flow rate, reach a maximum and then decrease with liquid flow rate. This may be explained considering that if the liquid which remains in the column after draining is collected at the particle-particle contact points, its amount depends on the number of contact points previously wetted by the liquid, and hence on the fluid flow rates. Figure 12 shows typical variation in β_s and when compared with the flow pattern of the phases indicates that the maximum in β_s occurs in pulse flow region.

The correlations for the pressure drop and liquid saturation developed in the present study cover the following range of experimental conditions:

$4.13 \le L \le 99.1$; $0.16 \le G \le 3.16$; $3.14 \le d_p \le 13.03$; $0.28 \le a_s \le 0.95$; $55 \le Re_l \le 1070$; $33 \le Re_g \le 1990$; $0.36 \le \epsilon \le 0.70$

The correlations as presented in terms of the Reynolds numbers based on the flow rates of the phases and packing characteristics possess the advantage of estimation of the aforementioned parameters directly instead through the single-phase pressure drops. Further, the correlations take into consideration the flow pattern of the phases and for the purpose the flow map due to Gianetto et al. (1978) is sufficiently accurate to delineate the flow regions *a priori* (Rao et al., 1981).

NOTATION

A-D = constants
a-e = constants
a_s = specific surface area of the bed, m^{-1}(= $6(1-\epsilon)/d_e$)
d_p = effective particle diameter, m
d_e = equivalent pore diameter, m(= $(2/3)[d_p\epsilon/(1-\epsilon)]$
G = superficial gas velocity, kg·m^{-2}·s^{-1}

g = acceleration due to gravity, $m \cdot s^{-2}$
ΔH = head loss, m $(= \Delta P/\rho g)$
h = height of packing, m
L = superficial liquid velocity, $kg \cdot m^{-2} \cdot s^{-1}$
ΔP = pressure drop, $N \cdot m^{-2}$
V = superficial velocity, $m \cdot s^{-1}$

Greek Letters

β = liquid holdup; subscript a refers to active (based or RTD); d = dynamic; i = within the pores of particles O = gross total; r = inactive (based on RTD); S = static; t = held in the interstices between the particles
ϵ = porosity
μ = viscosity, $kg \cdot m^{-1} \cdot s^{-1}$
ρ = density, $kg \cdot m^{-3}$
σ = surface tension, $N \cdot m^{-1}$, standard deviation

Dimensionless Parameters/Groups

$Bn = \rho_l g/\sigma a_s^2$, Bond number
$E\ddot{o} = \rho_l g d_p^2/\sigma$, Eötvos number
$Ga = d_p^3 g \rho^2/\mu^2$, Gallileo number
$Ga' = d_p^3 g \rho_l^2 (1 + \delta_{lg})/\mu_l^2$, modified Gallileo number
$Ga_l = \rho_l^3 g d_p^2 [1 - (g_c/\rho_l \beta_t g)(dp/dh)]\mu_l^2$
$Re = d_p V \rho/\mu$, Reynolds number
$Re_t = \rho_l V d_p/\mu_l (1 - \epsilon)(\beta_d/\beta_t)$
$We = V_g^2 d_e \rho_g/\sigma$, Weber number
$Z = Re_g^{1.167}/Re_l^{0.767}$
$\xi_g = (G/\epsilon)[(1/\rho_g)(\Delta H/\Delta h)_g + (1/\rho_w)]$
$\xi_l = (L/\epsilon)[(1/\rho_l)(\Delta H/\Delta h)_l + (1/\rho_w)]$
$\delta = (\Delta P/\rho g h)$
$\varphi_l = (\delta_{lg}/\delta_l)^{1/2}$
$\chi = (\delta_l/\delta_g)^{1/2}$
$\chi' = (\xi_l/\xi_g)^{1/2}$
$\psi = (\Delta P/{}^1/_2 \rho V^2)(d_p/h)$
$\eta = (1 - \epsilon)^2/\epsilon^3$
$\Delta = (\sigma_w/\sigma_l)[(\mu_l/\mu_w)(\rho_w/\rho_l)^2]^{1/3}$
$\lambda = [(\rho_g/\rho_{air})(\rho_l/\rho_w)]^{1/2}$

Subscripts

f = frictional
g = gas phase
l = liquid phase
lg = two-phase
w = water

Superscript

o = single phase

LITERATURE CITED

Beimesch, W. E., and D. P. Kessler, "Liquid-gas distribution measurements in the pulsing regime of two-phase concurrent flow in packed beds," *AIChE J.*, **17**, 1160 (1971).

Charpentier, J. C., "Recent progress in the phase gas-liquid mass transfer in packed beds," *Chem. Eng., J.*, **11**, 161 (1976).

Charpentier, J. C., and M. Favier, "Some liquid holdup experimental data in trickle bed reactors for foaming and non-foaming hydrocarbons," *AIChE J.*, **21**, 1213 (1975).

Charpentier, J. C., M. Bakos, and P. Le Goff, "Hydrodynamics of two-phase concurrent downflow in packed bed reactors", paper presented at the 2nd Congr. on 'Quelques applications de la Chimie physique," Veszprem, Hungary (1971).

Charpentier, J. C., C. Prost, and P. Le Goff, "Chute de pression pour des ecoulements a co-current et a contrecourant dans les collonnes a garnissage arrose: Comparaison avee le garnissage noye," *Chem. Eng. Sci.*, **24**, 1777 (1969).

Charpentier, J. C., C. Prost, W. Van Swaaiji, and P. Le Goff, "Etude de la retention de liquide dans une ecolonne a granissage arrose a co-current et a contre-courant de gaz-liquide," *Chimie et Industrie, Genie Chimie et Industrie, Genie Chimique*, **99**, 803 (1968).

Clements, L. D., "Dynamic liquid holdup in cocurrent gas-liquid downflow in packed beds," "Two-phase Transport and Reactor Safety," T. N. Veziroglu and S. Kakac, eds., Hemisphere Publ. Corp., Washington, 69 (1978).

Clements, L. D., and P. C. Schmidt, "Two-phase pressure drop in cocurrent downflow in packed beds: Air silicone oil Systems," *AIChE J.*, **26**, (2), 314 (1980a).

Clements, L. D., and P. C. Schmidt, "Dynamic liquid holdup in two phase downflow in packed beds: Air silicone oils system, *AIChE J.*, **26**, (2), 317 (1980b).

Dodds, W. S., L. F. Stutzman, B. J. Sollami, and R. J. McCarter, "Pressure drop and liquid holdup in concurrent gas absorption," *AIChE J.*, **6**, 390 (1960).

Gianetto, A., G. Baldi, V. Specchia, and S. Sicardi, "Hydrodynamics and solid-liquid contacting effectiveness in trickle-bed reactors," *AIChE J.*, **24**, 1087 (1978).

Goto, S., and J. M. Smith, "Trickle-bed reactor performance Part-I: Holdup and mass transfer effects," *AIChE J.*, **21**, 706, 714 (1975).

Hochman, J. M., and E. Effron, "Two-phase cocurrent downflow in packed beds," *Ind. Eng. Chem., Fund.*, **8**, 63 (1969).

Hirose, T., "Recent trend of studies on gas-liquid cocurrent packed column," Symposium on "Multiphase concurrent fixed beds," Okayama, 1 (1978).

Hofmann, P. H., "Multiphase catalytic packed-bed reactors," *Catl. Rev.-Sci. Eng.*, **17**, 71 (1978).

Larkins, R. P., "Two-phase concurrent flow in packed beds," Ph.D. Thesis, Univ. of Michigan (1959).

Larkins, R. P., "Two-phase concurrent flow in packed beds," Ph.D. Thesis, Univ. of Michigan (1959).

Larkins, R. P., R. R. White, and D. W. Jeffrey, "Two-phase concurrent flow in packed beds," *AIChE J.*, **7**, 231 (1961).

Lockhart, R. W., and R. C. Martinelli, "Proposed correlation of data for isothermal two-phase, two-component flow in pipes," *Chem. Eng. Prog.*, **45**, 39 (1949).

Matsuura, A., T. Akehata, and T. Shirai, "Friction factor of gas-liquid concurrent downflow through packed beds," *Kagaku Kogaku Ronbunshu*, **3**, (2), 122 (1977).

Matsuura, A., T. Akehata, and T. Shirai, "Flow pattern of cocurrent gas-liquid downflow in packed beds," *Kagaku Kogaku Ronbunshu*, **5** (2), 167 (1979).

Mersmann, A., "Die trennwirkung von Hohlfüllkörpern," *Chemie-Ing. Techn.*, **37**, 672 (1965).

Mersmann A., "Fluid dynamics of fluid two-phase system," *Int. Congr. Chem. Eng. Equip. Des. Autom.* (*Process*), Prague, 12.1 (1975).

Midoux, N., M. Favier, and J. C. Charpentier, "Flow pattern, pressure loss and liquid holdup data in gas-liquid downflow packed beds with foaming and non-foaming hydrocarbons," *J. Chem. Eng. Japan*, **9**, 350 (1976).

Morsi, B. I., N. Midoux, and J. C. Charpentier, "Flow patterns and some holdup experimental data in trickle-bed reactors for foaming, non-foaming and viscous organic liquids," *AIChE J.*, **24**, 357 (1978).

Otake, T., and K. Okada, "Liquid holdup in packed towers," *Kogaku Kogaku (ChemEngng. Japan)*, **17**, 176 (1953).

Raju, R. S., "Hydrodynamic studies in trickle bed reactors," M.S. Thesis, IIT Madras (1979).

Rao, V. G., "Study of the pressure drop and liquid holdup in gas-liquid concurrent downflow through packed beds," Ph.D. Thesis, IIT Madras (1979).

Rao, V. G., R. S. Raju, M. S. Ananth, and Y. B. G. Varma, "Flow pattern in cocurrent gas-liquid downflow in packed beds," *Trans. Ind. Chem. Engr.*, **23**, T 25 (1981).

Sato, Y., T. Hirose, F. Takahashi, and M. Toda, "Pressure loss and liquid holdup in packed bed reactor with cocurrent gas-liquid downflow," *J. Chem. Eng. Japan*, **6**, 147 (1973).

Satterfield, C. N., "Trickle-bed reactors," *AIChE J.*, **21**, 209 (1975).

Satterfield, C. N., and F. Way, "The role of liquid phase in the performance of a trickle bed reactor," *AIChE J.*, **18**, 305 (1972).

Schwartz, J. G., E. Weger, and M. P. Dodukovic, "Liquid holdup and dispersion in trickle-beds," *AIChE J.*, **22**, 153 (1976).

Shah, Y. T., G. J. Stiegel, and M. M. Sharma, "Backmixing in gas-liquid reactors," *AIChE J.*, **24**, 369 (1978).

Specchia, V., and G. Baldi, "Pressure drop and liquid holdup for two-phase concurrent flow in packed beds," *Chem. Eng. Sci.*, **32**, 515 (1977).

Talmor, E., "Two-phase downflow through catalyst beds," *AIChE J.*, **23**, 868 (1977).

Turpin, J. L., and R. L. Huntington, "Prediction of pressure drop for two-phase two-component concurrent flow in packed beds," *AIChE J.*, **13**, 1196 (1967).
Van Landeghem, H., "Multiphase reactors: Mass transfer and modelling," *Chem. Eng. Sci.*, **35**, 1912 (1980).
Weekman, Jr., V. W., and E. Myers, "Fluid flow characteristics of concurrent gas-liquid flow in packed beds," *AIChE J.*, **10**, 951 (1964).
Wen, C. Y., O'Brien, and L. T. Fan, "Pressure drop through packed beds operated cocurrently," *J. Chem. Eng. Data*, **8**, 48 (1963).

Manuscript received October 31, 1981; revision received May 3, and accepted May 28, 1982.

Effect of Interfacial Viscosities upon Displacement in Capillaries with Special Application to Tertiary Oil Recovery

Washburn's equation has been generalized to explain the relative effects of the interfacial viscosities, interfacial tension, and wetting during displacement in a single, cylindrical capillary. The effect of the interfacial viscosities is to increase the resistance to displacement regardless of the wetting condition. The predictions of a prior qualitative theory for the relative effects of the interfacial viscosities and of interfacial tension during tertiary oil recovery are fully supported by this analysis. This discussion further indicates that the interfacial dilatational viscosity may be relatively more important than the interfacial shear viscosity.

R. M. GIORDANO and J. C. SLATTERY

Department of Chemical Engineering
Northwestern University
Evanston, IL 60201

SCOPE

Conventional production of light crudes usually concludes with a partial displacement of the oil remaining in the reservoir by either water or brine. The void volume in a permeable rock, such as that in which oil is found, may be thought of as many intersecting pores of varying diameters. Consider two neighboring pore networks having different mean radii that offer parallel paths for displacement. Oil (residual oil) will be trapped in that pore network through which the oil is displaced more slowly. For carefully selected, well-designed, good performing operations, at the end of conventional petroleum production there remains trapped in this way 50–70% of the oil originally in place (Geffen, 1973).

Slattery (1974, 1979) developed a qualitative theory for the relative effects of interfacial tension, the interfacial viscosities, and wetting upon the displacement of this residual oil. He concludes that, when the interfacial tension is less than the critical value required for displacement and when the interfacial viscosities are large, the rate of displacement will be adversely affected by the interfacial viscosities.

There are no experimental data that either support or reject this theory.

The objective in what follows is to test this theory by developing a more complete, quantitative analysis for the relative effects of the interfacial viscosities, interfacial tension, and wetting during displacement in a single, cylindrical pore.

CONCLUSIONS AND SIGNIFICANCE

Washburn's (1921) equation has been generalized to include the effects of the interfacial viscosities. The result is limited by assumptions that the Reynolds number N_{Re}, the capillary number N_{ca}, and the Bond number N_{Bo} are all small compared with unity and that surface viscous forces dominate bulk viscous forces in the interface (the dimensionless sum of the interfacial viscosities $N_{\kappa+\epsilon} \gg 1$).

The limited data available for the interfacial viscosities of proposed tertiary oil recovery systems indicate that the dimensionless sum of the interfacial viscosities $N_{\kappa+\epsilon} \gg 1$.

Tertiary oil displacements would normally be conducted with relatively constant pressure differences between injection and production wells. The effect of the interfacial viscosities is to decrease the speed of displacement for a given pressure drop regardless of the wetting condition. Of the two interfacial viscosities, the interfacial dilatational viscosity may play the dominant role. This suggests that for a successful tertiary oil recovery system the interfacial viscosities, particularly the interfacial dilatational viscosity, should be as small as possible.

The conclusion of Slattery's (1974, 1979) qualitative theory for the effects of the interfacial viscosities in tertiary oil recovery is fully supported by this quantitative analysis, although this discussion further indicates that the interfacial dilatational viscosity may be relatively more important than the interfacial shear viscosity.